Impact of measurement parameters on antenna radiation pattern reconstruction using phaseless iterative technique

Myssipsa Mehraz, François Gallée

Impact of measurement parameters on antenna radiation pattern reconstruction using phaseless iterative technique

Myssipsa Mehraz
Microwave department – IMT Atlantique
Lab-STICC CNRS UMR 6285
Brest, France
myssipsa.mehraz@imt-atlantique.fr

François Gallée
Microwave department – IMT Atlantique
Lab-STICC CNRS UMR 6285
Brest, France
francois.gallee@imt-atlantique.fr

***Abstract*— This study focuses on the impact of planar near-field measurement parameters, such as plane size, sampling step and the distance between the Antenna Under Test (AUT) and the measurement plane. The main objective of this work is to determine the optimal near-field measurement parameters that achieve an assessment of far-field (FF) radiation pattern accuracy versus measurement duration.**

Keywords*— *Nearfield measurements, Antenna characterization, Iterative Fourier Technique, Phaseless techniques, Radiation pattern reconstruction Introduction (Heading 1)

I. INTRODUCTION

Near-field antenna characterization methods offer an alternative to direct far-field measurements but often necessitate considerable data acquisition and both amplitude and phase measurements for subsequent near-to-far-field transformations. Phaseless techniques have emerged as a practical alternative to these traditional methods and offer several advantages, such as the ability to eliminate the need of expensive equipment and highly precise positioning systems [1]. Additionally, they hold the promise of simplifying OTA (Over-The-Air) for devices without direct access to the antenna. The most commonly used technique in this type of measurement is called the Iterative Fourier Technique (IFT) [2], which is based on propagating the measured amplitude between two surfaces, located at different distances from the antenna aperture using plane wave spectrum in order to reconstruct the phase and then apply a traditional near-field to far-field transformation.

The parameters that the user must define for a standard planar near-field measurement are the size of the measurement plane, the distance separating the Antenna Under Test (AUT) and the measurement plane, and the sampling step. In theory, for complete and precise reconstruction, the measurement plane should be infinite in size, and the sampling step should be as small as possible to capture all variations in the electric field on this plane. In practice, the plane is truncated from infinity, and the sampling step is calculated while respecting Nyquist's condition. Furthermore, the required separation distance between the AUT and the measurement plane is determined by the reactive field radiated.

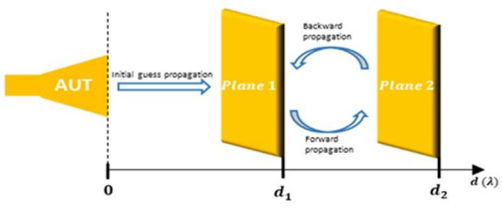

Fig. 1. Phaseless measurement principle

The Phaseless Iterative Fourier Technique (IFT)starts with an initial guess of phase and amplitude across the antenna's aperture. Then, it propagates this initial distribution towards Plane 1 using Plane Wave Spectrum (PWS) theory. Here, the propagated amplitude is replaced with the actual measured one, while the phase is retained. This process repeats forward (from Plane 1 to Plane 2) and backward (from Plane 2 to Plane 1), updating the propagated amplitude with the real measurements on each plane. The phase is adjusted on each iteration and it keeps iterating until a predefined error rate or when a maximum number of iterations is reached.

The parameters addressed in this study for planar near-field measurement using phaseless IFT method are the size of the measurement plane, the distance separating the Antenna Under Test (AUT) and the measurement plane, the sampling step. The main objective of this work is to contribute to the specification of near-field measurement parameters that achieve an assessment of far-field (FF) radiation pattern accuracy versus measurement duration.

II. DEFINE OPTIMAL MEASUREMENT PARAMETERS

A. Measurement plane size and distance for the AUT

Firstly, to establish the optimal near-field measurement parameters regarding the desired radiation pattern cutoff angle, a criterion (Fig. 2) has been empirically established through extensive measurements [2] and substantiated through theoretical analysis [3]. It could be used to determine the minimum size of the scan plane for a given desired angular region of coverage and the distance d between the aperture of the antenna and the measurement plane.

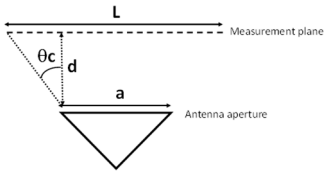

Fig. 2. Critical cutoff angle (θc)

$$\theta_c = Atan\left(\frac{L-a}{2d}\right) \qquad (1)$$

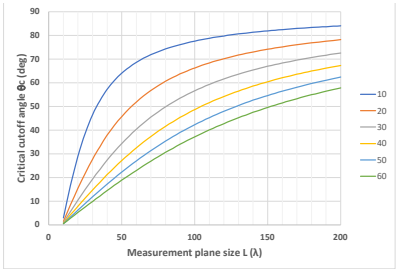

Fig. 3. Critical cutoff angle (θc) versus measurement plane size (L) for differents distance (d)

The curves on the fig. 3 show that this criterion is very restrictive but necessary if very small measurement error is wanted over a large angle range. In our case, to optimise the size of the measurement, an amplitude range from the maximum amplitude will be defined, for example (30dB). Outside, the measurement plane size could be increase by filling null value.

The optimal distance d of the measurement planes from the antenna aperture should be in the Rayleigh zone to avoid the reactive where strong coupling effect between the AUT and the probe could disturb the measurement. Our test bench "caronchip" is presented on the fig.4. On the fig. 5, the evolution of the electric field amplitude measured and simulated above a rectangular horn antenna at 96GHz along vertical axis, allows firstly to validate your test bench and from the antenna aperture size to define the optimal distance of the measurement planes. The first plane will be located at the end of the reactive in order to minimise the measurement plane size. In the case of the horn antenna, the distances of measurement planes should be selected between 24λ and 64λ.

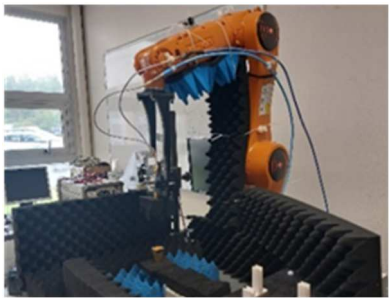

Fig. 4. "Caronchip" test bench

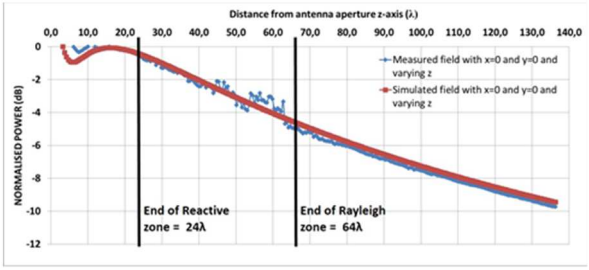

Fig. 5. Evolution of the amplitude in the near field zone

B. Spatial sampling

Once the measurement plane size and the distance are optimized, the measurement duration depend on the number of measurement point. The general rule is to fix a half wavelength spatial sampling without angle restriction. It is possible to increase the spatial sampling but with an impact about the angle range and the goal is to evaluate it.

The spatial sampling effect could be study from the theory of PWS [2]. The electric field is written as follows :

$$E(x,y,z) = \frac{1}{4\pi^2}\iint_{-\infty}^{+\infty}\left[F_x(k_x,k_y)\hat{x} + F_x(k_x,k_y)\hat{y} + F_z(k_x,k_y)\hat{z}\right] e^{-j\left(k_x x + k_y y + \sqrt{k0^2 - k_x^2 - k_y^2}z\right)} dk_x dk_y \qquad (2)$$

With

$$\left(k_x x + k_y y + \sqrt{k_0^2 - k_x^2 - k_y^2}z\right) = k.r \qquad (3)$$

And

$$k_0 = \frac{2\pi}{\lambda} \qquad (4)$$

The radiation condition in 3D requires that for $z \geq 0$, the relation between wavenumbers should ensure:

$$k_z = \begin{cases} \left(k^2 - k_x^2 - k_y^2\right)^{\frac{1}{2}} & \text{if } k_x^2 + k_y^2 \leq k^2 \\ -j\left(k^2 - k_x^2 - k_y^2\right)^{\frac{1}{2}} & \text{otherwise} \end{cases} \qquad (5)$$

The method of stationary phase is used to derive easy-to-use formula far field calculations.

$$\frac{\partial k.r}{\partial k_x} = \frac{\partial k.r}{\partial k_y} = 0 \qquad (6)$$

The solution to (5) is:

$$k_x = k_0 \sin\theta\cos\varphi \qquad (7)$$

$$k_y = k_0 \sin\theta\sin\varphi \qquad (8)$$

Where θ and ϕ represent the angles associated with the spherical coordinate system: θ is the elevation angle, and ϕ is the azimuth angle.

The wavenumbers k_x and k_y can be written in the Cartesian domain as:

$$k_x = \frac{2\pi m}{M\Delta_x} \qquad (9)$$

$$k_y = \frac{2\pi n}{N\Delta_y} \qquad (10)$$

With Δ_x and Δ_y the sampling steps following respectively the x and y-axis. M and N are the maximum number of samples. In addition, m and n index to the positions in the scan plane as:

$$-\frac{M}{2} \leq m \leq \frac{M}{2} \qquad (1)$$

$$-\frac{N}{2} \leq n \leq \frac{N}{2} \qquad (2)$$

Let us now deduce the sampling step from the previous equations. We'll show the development only for k_y as the calculation is the same for k_x.

By replace in (6) $\varphi = 90°$ for the far-field E plane, the maximum farfield cutoff $\theta_{FF_{MAX}}$ is obtained for

$$k_{y_{MAX}} = \frac{\pi}{\Delta_x} \qquad (3)\,.$$

$$\theta_{FF_{MAX}} = \sin^{-1}\left(\frac{k_{y_{MAX}}}{k_0}\right) \qquad (4)$$

Thus

$$\theta_{FF_{MAX}} = \sin^{-1}\left(\frac{\lambda}{2\Delta_y}\right) \qquad (15)$$

The curves Fig 6. illustrates the spatial sampling step as a function of the desired far-field cutoff angle respectively when there's no aliasing.

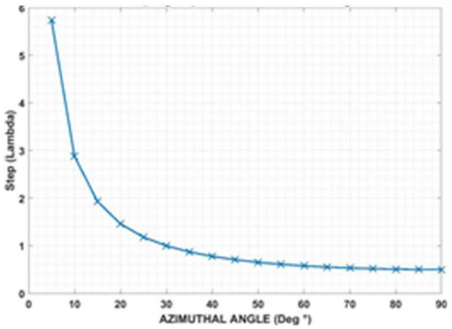

Fig. 6. Sampling step function of desired FF cutoff angle

Fig 7. and 8. Shows respectively radiation pattern for the E and H plane of a 96 GHz horn antenna, computed using near-field data simulated in FEKO for various sampling steps computed. Plane size is about 256 λ

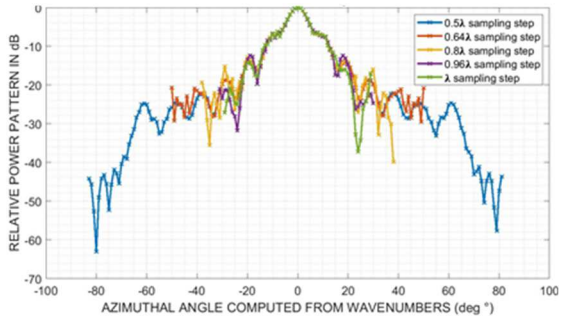

Fig. 7. Radiation pattern - E Plane

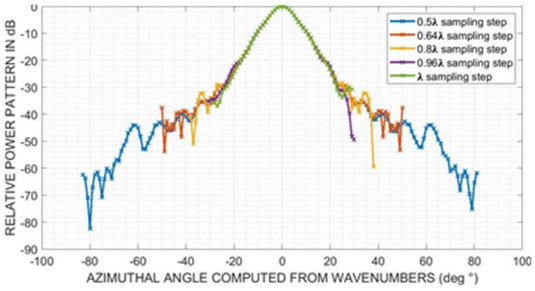

Fig. 8. Radiation pattern - H plane

As mentioned earlier, equation (15) provides a theoretical result different from practical observations. Indeed, Fig 9 illustrates the discrepancy compared to the case with a spatial sampling step of 0.5 lambda, as recommended by Nyquist. The error increases when the spatial sampling increase.

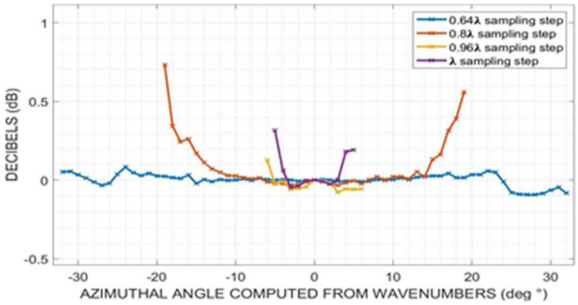

Fig. 9. Difference between reference PWS for 0.5 lambda step and for greater steps – E PLANE

Table 1. shows a comparison between calculated cutoff angle from (fig.6) and obtained angle from y axis Plane Wave Spectra in E plane with a maximum error of 0.1dB.

TABLE I. COMPARISON BETWEEN SUPPOSED CUTOFF ANGLE AND OBTAINED ONE

NF Sampling step	E PLANE	
	Supposed	Obtained
0.64 λ	51.37°	32°
0.8 λ	38.68°	19°
0.96 λ	31.88°	10°
1 λ	30°	10°

The difference between supposed and obtained azimuthal angles is due to aliasing after Fourier transform in NF to FF algorithm that depends on the crossing point between the central spectrum and the first spectra repeated to the left, and right of it. During aliasing, some of the secondary spectra overlap with the main spectrum, resulting in distortions of the reconstructed spectrum as shown in Fig 13. An assessment of the aliasing impact depending on the electric field distribution should be taking into account to avoid or control the error.

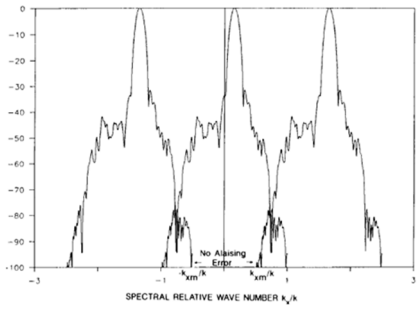

Fig. 10. Illustation of aliasing error due to overlapping of offset spectra (C.NEWELL, 1988)

III. IFT Method Validation

The IFT (Iterative Fourier Transform) method allows measurements to be made in amplitude only and then reconstructs the phase through an iterative process between the two measurement surfaces.

Before starting this iterative process, it's crucial to choose an initial distribution of amplitude and phase across the antenna aperture. While amplitude is usually set to 1 across all points on the aperture special attention is needed when setting the initial phase, as it impacts whether the iterative algorithm successfully converges to a global solution and influences the convergence time. Three main methods were developed for IFT initial guess and presented in [4]. In our study, we use the "Basic Approach" for the initial guess that defines constant phase and ones for amplitudes across the antenna aperture.

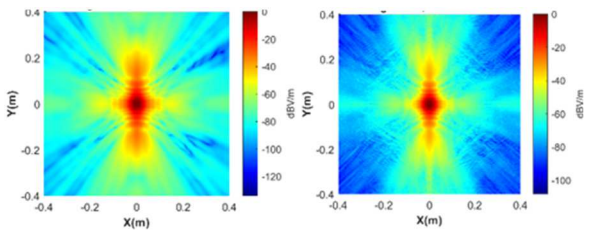

Fig. 11. theoretical (left) and reconstructed (right) magnitude using ITF d1 = 24λ d2 = 45λ

To validate the implementation of the IFT, Fig.11 and Fig.12 show the magnitude and phase correctly reconstructed with only near field planes amplitude data taken from FEKO simulatio, with a maximum in the plane center of 26.3128 dBV/m for theoretical plane and 26.2815 dBV/m for reconstructed one.

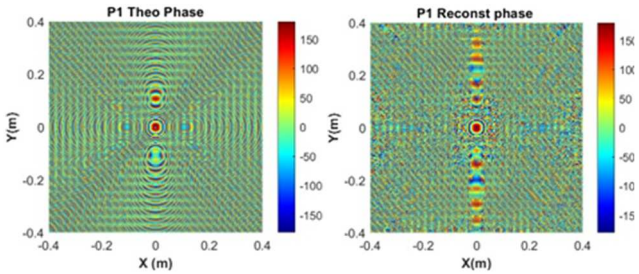

Fig. 12. Theoretical phase (left) and reconstructed phase (right) using ITF

Fig 13. depicts the relationship between the amplitude error and phase difference according to the electric field magnitude between theoretical and reconstructed amplitudes and phases. It is evident that the error is concentrated in regions with low field magnitude and allow to validate the measurement. These plots could be very interesting to define a criterion during the iterative process of the ITF.

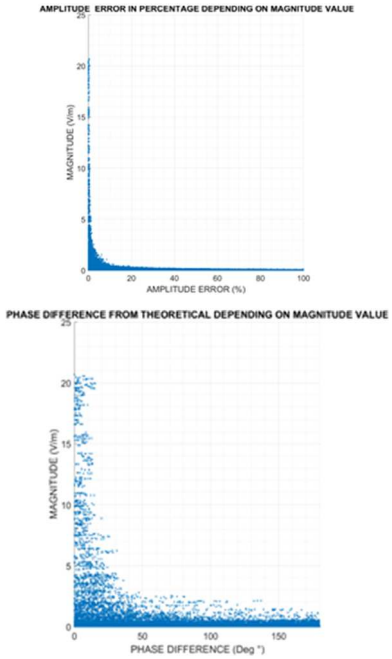

Fig. 13. Amplitude and phase difference between theoretical and reconstructed field

The measured radiation pattern computed with a spatial sampling of 0.64 and compare to the simulated radiation pattern in E plane is showed in the Fig.14. The blue and red curves are the measurement at two distances plane measurement. In this plane, the aliasing error is present. This can be explained by uniform distribution of the field in the antenna aperture. In the H plane, Fig.15, there is no aliasing error because the electric filed distribution in this plane is a cosinus distribution. The difference between the simulated and the measurement is due to the measurement test bench sensitivity.

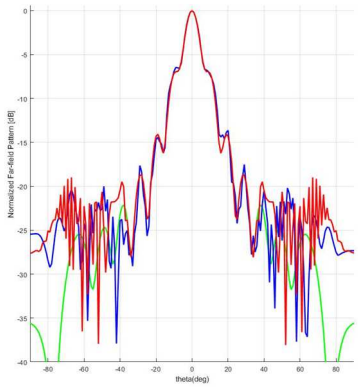

Fig. 14. Measured (Blue and red) and simulated (green) radiation pattern in the E plane.

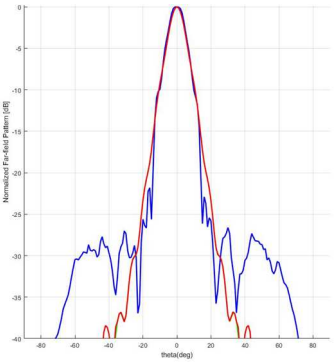

Fig. 15. Measured (Blue) and simulated (red) radiation pattern in the E plane.

IV. Conclusion and Perspectives

In this paper, the impact of the nearfield antenna measurement parameters has been studied with the definition of primary rules to optimize the measurement duration according to the angle range and the error. Depending on the expected antenna parameters, for example, 3dB beamwidth, first side lobes level, it's possible to increase the spatial sampling to reduce the measurement duration

The future work will be to test these different criteria from different antenna radiation pattern to validate them and propose technics like interpolation or non-uniform mesh of measurement points.

References

[1] S. F. Razavi et Y. Rahmat-Samii, « Resilience to Probe-Positioning Errors in Planar Phaseless Near-Field Measurements », IEEE Trans. Antennas Propag., vol. 58, no 8, p. 2632-2640, août 2010, doi: 10.1109/TAP.2010.2050421.

[2] A. D. Yaghjian, « Upper-bound errors in far-field antenna parameters determined from planar near-field measurements : PART 1: analysis ».

[3] A. C. Newell et M. L. Crawford, « Planar near-field measurements on high performance array antennas », National Bureau of Standards, Gaithersburg, MD, NBS IR 74-380, 1974. doi: 10.6028/NBS.IR.74-380.

[4] X. Li, « Investigation of the Iterative Fourier Technique for Phaseless Planar Near-Field Antenna Measurements ».

[5] A. C. Newell, « Error analysis techniques for planar near-field measurements », IEEE Trans. Antennas Propag., vol. 36, no 6, p. 754-768, juin 1988, doi: 10.1109/8.1177.

[6] E. Joy et D. Paris, « Spatial sampling and filtering in near-field measurements », IEEE Trans. Antennas Propag., vol. 20, no 3, p. 253-261, mai 1972, doi: 10.1109/TAP.1972.1140193.